Idaho Incubation Fund Program

Final Report Form

Proposal No.	IF13-003
Name:	An Chen and Richard Nielsen
Name of Institution:	University of Idaho
Project Title:	Development of an Energy Efficient Integrated FRP-confined Precast Concrete Sandwich Roof Panel for Green Buildings

Information to be reported in your final report is as follows:

1. Provide a summary of overall project accomplishments to include goals/milestones met, any barriers encountered, and how the barriers were overcome:

1.1 Project goals/milestones:
- Finite Element (FE) models to simulate insulated precast concrete sandwich panels.
- Bending tests on scaled specimens.
- Bending tests on full-scale specimens.
- Creep tests on scaled specimens.
- Business plan development.

1.2 Accomplishments:

1.2.1 Finite Element (FE) models to simulate insulated precast concrete sandwich panels:

Linear and nonlinear finite element analysis (FEA) models were created using ABAQUS© which is a commercially available numerical solver. The models were created in ABAQUS using CAE interface and then solved in ABAQUS with its own solver. The linear and nonlinear properties of the materials were incorporated into the FE models and the DAMAGED PLASTICITY function for nonlinear engineering material property of the concrete was utilized. By using this feature in ABAQUS the numerical model can account for the loss of stiffness of the elements in compression and tension when the limit of cracking and crushing strains are exceeded.

Table 1: Material properties for insulation

ASTM C578	Expanded Polystyrene	Extruded Polystyrene
Mass Density (ρ)	1.871 x 10^{-6} (lbf s^2)/in^4	2.994 x 10^{-6} (lbf s^2)/in^4
Young's Modulus (E)	1,349 psi	1,349 psi
Shear Modulus (G)	400 psi	400 psi
Tensile Strength (Fu)	20 psi	50 psi
Poisson's Ratio (ν)	0.3	0.3

Table 2: Material properties for concrete

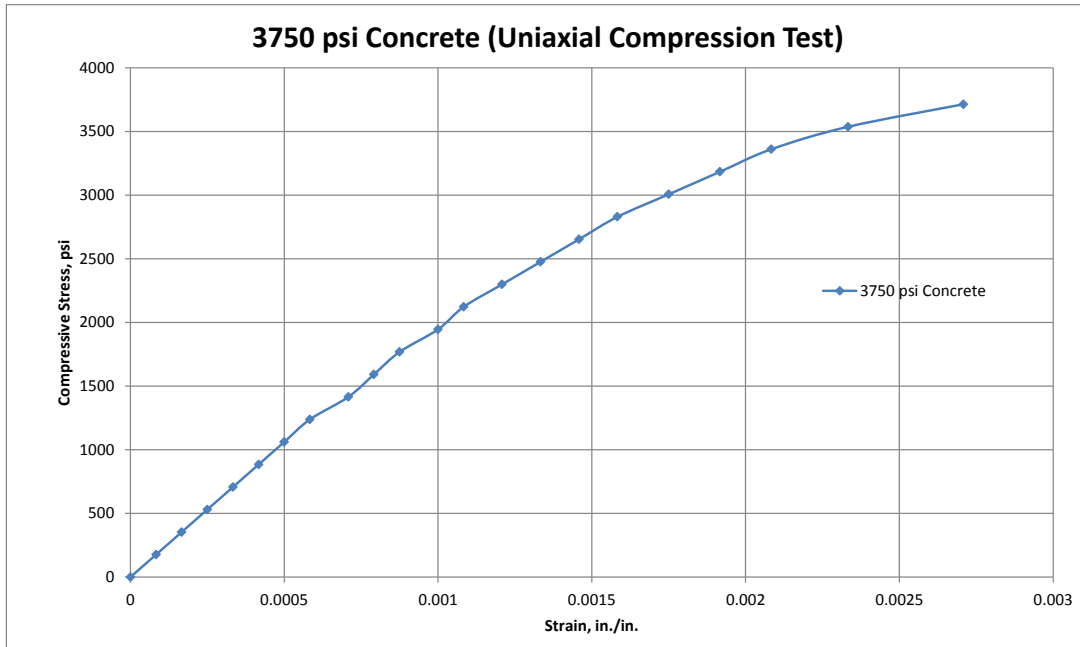|	5000 psi Concrete	3750 psi Concrete
Volume Density (γ)	150 lbf/ft^3	150 lbf/ft^3
Mass Density (ρ)	2.246 x 10^{-4} (lbf s^2)/in^4	2.246 x 10^{-4} (lbf s^2)/in^4
Young's Modulus (E)	4.031 x 10^6 psi	2.558 x 10^6 psi
Poisson's Ratio (ν)	0.15	0.15
Modulus of Rupture (fr)	530 psi	459 psi

Figure 1: Stress strain properties of uniaxial compression test

Material properties for insulation and concrete are shown in Tables 1 and 2, respectively. A 6" diameter by 12" tall concrete cylinder sample was obtained during the initial pour of the scaled test panels in November, 2012 and tested at the 28 day time interval at Washington State University testing labs for the Phase I testing. The cylinders were tested in accordance with ASTM C39 for compressive strength and the static modulus of elasticity and Poisson's ratio of the concrete in compression was obtained in accordance with ASTM C469/C469M-10 (2010). Further test cylinders were fabricated and tested in the University of Idaho structures lab in the summer of 2013 for the Phase II testing. Figure 1 shows the stress strain data for the Phase I cylinders and Figure 2 shows the actual test data of the specimens.

Sample type (6"x 12" cylinder)		Date	12/13/2012		
Loading force (lbs.)		1st Reading	2nd Reading	Strain	Stress
0		0	0	0	0
5000		0.0005	0.001	8.33333E-05	176.8388
10000		0.002	0.002	0.000166667	353.6777
15000		0.003	0.003	0.00025	530.5165
20000		0.0035	0.004	0.000333333	707.3553
25000		0.005	0.005	0.000416667	884.1941
30000		0.006	0.006	0.0005	1061.033
35000		0.0075	0.007	0.000583333	1237.872
40000		0.0085	0.0085	0.000708333	1414.711
45000			0.0095	0.000791667	1591.549
50000			0.0105	0.000875	1768.388
55000			0.012	0.001	1945.227
60000			0.013	0.001083333	2122.066
65000			0.0145	0.001208333	2298.905
70000			0.016	0.001333333	2475.744
75000			0.0175	0.001458333	2652.582
80000			0.019	0.001583333	2829.421
85000			0.021	0.00175	3006.26
90000			0.023	0.001916667	3183.099
95000			0.025	0.002083333	3359.938
100000			0.028	0.002333333	3536.777
105000			0.0325	0.002708333	3713.615

ASTM C469 Std Test Method for Static Modulus of Elasticity and Poisson's Ratio of Concrete					
Ultimate load		106182	106182		
40% Ultimate load		42472.8	42472.8		
nearest 40% load S2		40000	40000		
40% Ultimate load strain E2		0.00053125	0.00053125		
5*10-5 strain load S1		5000	5000		
5*10-5 strain E1 (Reading/2/12)*		2.0833E-05	4.16667E-05		
Young's modulus(psi)		2425218.18	2528418.954		
Young's Modulus (final)	Ec =	2476818.567		psi	
Compressive Strength:	f'c =	3755.42		psi	

Figure 2: Concrete compressive test data

In Phase 1 testing the tensile properties of the concrete material was created using an approximate 7% ratio of the compressive stress-strain data. Figure 3 shows the stress-strain curve of the tensile properties for the concrete material.
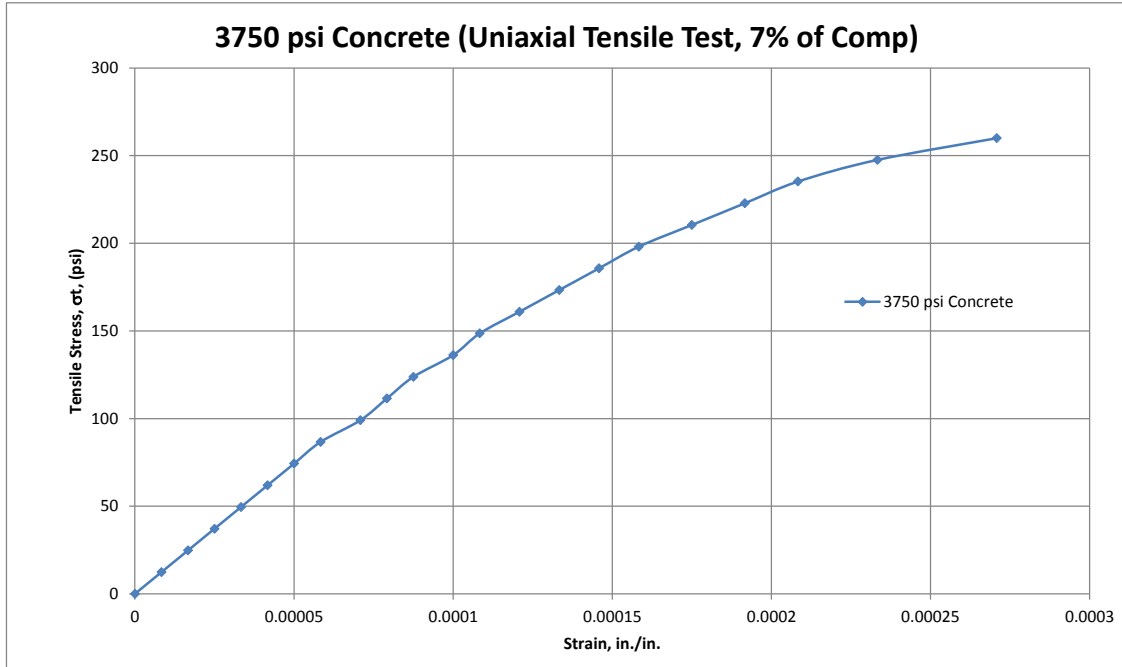
Figure 3: Corresponding estimate uniaxial tensile properties of concrete

In order to properly represent the structure in the FE model, the material properties of the structural elements should be attained prior to every discrete analysis. This will become unrealistic and difficult to accomplish, therefore without test data the estimated concrete material properties can be accurately derived by the following formulas derived by Mander et al. (1988).

The analytical model of the concrete in compression can be best described by:

$$f_c = \frac{f_{cc}' x r}{r - 1 + x'} \tag{1-1}$$

where f'$_{cc}$ = compressive strength of confined concrete.

$$x = \frac{\varepsilon_c}{\varepsilon_{cc}} \tag{1-2}$$

where ε_c = longitudinal compressive concrete strain

$$\varepsilon_{cc} = \varepsilon_{co}\left[1 + 5\left(\frac{f_{cc}'}{f_{co}'} - 1\right)\right] \tag{1-3}$$

generally ε_{co} = 0.002 can be assumed, and

$$r = \frac{E_c}{E_c - E_{sec}} \tag{1-4}$$

where

$$E_c = 57,000\sqrt{f_{co}'}\, psi \tag{1-5}$$

Which is the tangent modulus of elasticity of the concrete, and

$$E_{sec} = \frac{f_{cc}'}{\varepsilon_{cc}} \tag{1-6}$$

Without actual test data for the compressive and tensile properties of the concrete material the stress-strain curve can be created using the aforementioned equations and Figure 4 shows the comparison between the actual test data for the stress-strain curve and the theoretical. The curves match fairly well and can be used in the FE model.
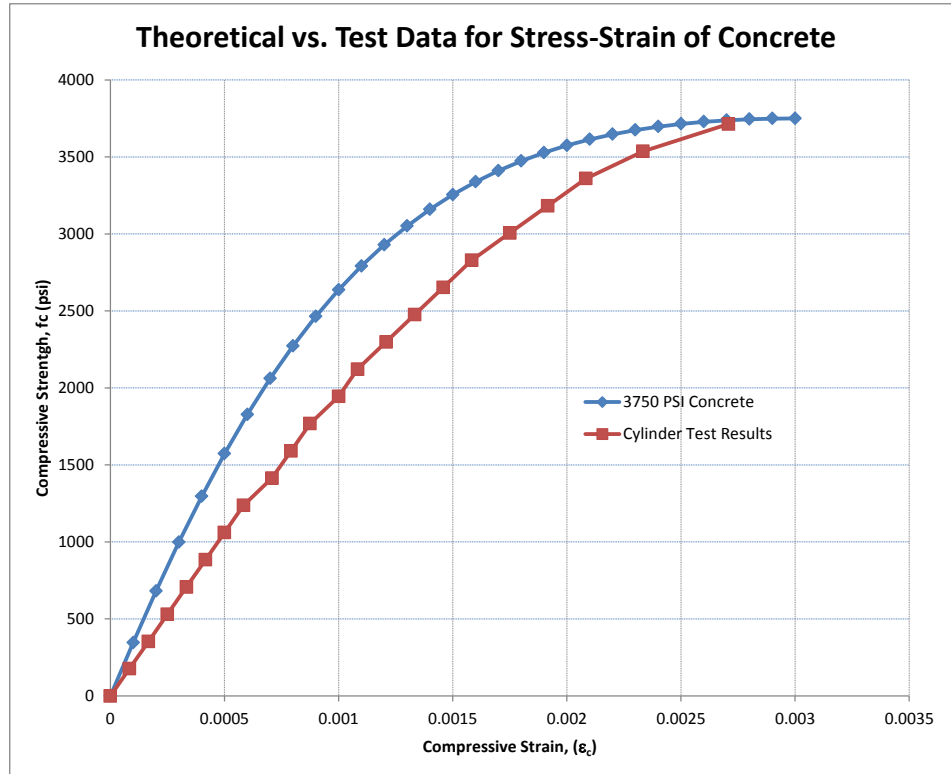

Figure 4: Theoretical vs. test data for concrete stress-strain curve

Using the model developed by Menegotto and Pinto (1973) the stress-strain properties of the reinforcing steel can be described by the following equation:

$$f_s = \frac{E_s \varepsilon_s}{\left[1 + \left(\frac{E_s \varepsilon_s}{f_y}\right)^{20}\right]^{0.05}} + \left(f_{su} - f_y\right)\left[\left(\frac{1 - \left(\varepsilon_{su} - \varepsilon_s\right)^p}{\varepsilon_{su} - \varepsilon_{sh}}\right)^{20p} + \left(\varepsilon_{su} - \varepsilon_s\right)^{20p}\right]^{0.05} \tag{1-7}$$

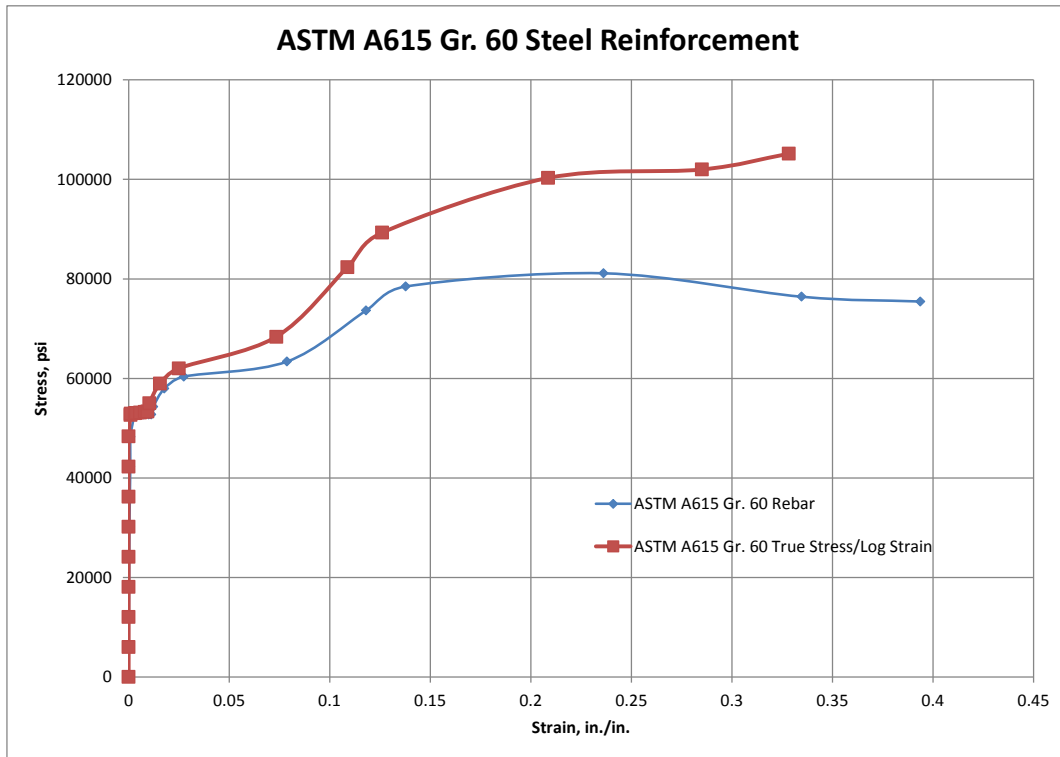$$p = E_{sh}\left(\frac{\varepsilon_{su} - \varepsilon_{sh}}{f_{su} - f_y}\right) \tag{1-8}$$

Figure 5: True stress-strain properties of ASTM A615 Gr. 60 steel

ABAQUS offers two modeling techniques for nonlinear concrete FE analysis. The first model is called concrete smeared cracking model and the second available plastic analysis model is concrete damaged plasticity model. The concrete smeared cracking model has been developed by Crisfield (1986), Hillerborg & Petersson (1976) and Kupfer & Gerstle (1973). The model works best for monotonic loading for concrete beams where the compressive strength of the concrete material along with the corresponding plastic strain is incorporated into the analysis model material properties. This particular model would seem to be the best choice for the type of analysis performed on the test panels. However, there were some difficulties in getting the analytical data and the test data to match well. Instead, the concrete damaged plasticity model was used for the FE modeling as it incorporated both the compressive and tensile properties of the concrete material and corresponding stiffness degradation values or damaged parameters could be used. The concrete damaged plasticity model is best used for concrete specimens that would experience cyclic loading as the material properties allow for stiffness recovery as cracks close and open for both tensile and compressive values.

The concrete damaged plasticity model was developed by ABAQUS based on research by Lubliner et al. (1989) and Lee & Fenves (1998). Although the test panels in this research work are not cyclically loaded, the capturing of stiffness degradation and damage to the concrete as the concrete either cracks in tension or crushes in compression is well defined and useful in the comparison of the FEA vs. Test data. As the concrete specimen is unloaded, the unloading response is said to be weakened

when observing any one point on the stress-strain curve. The degradation of this stiffness in tension and compression is characterized by Figure 6 and Figure 7 respectively.
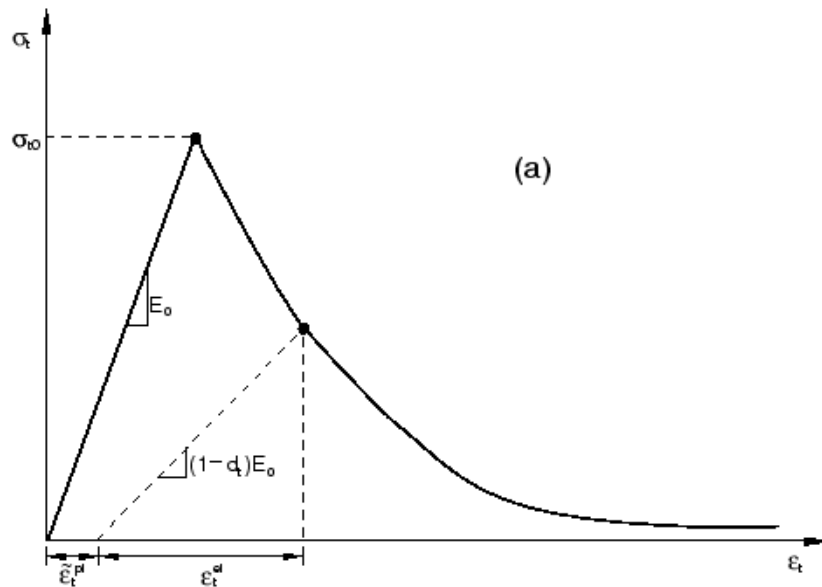

Figure 6: Response of concrete to uniaxial loading in tension (ABAQUS 2013)
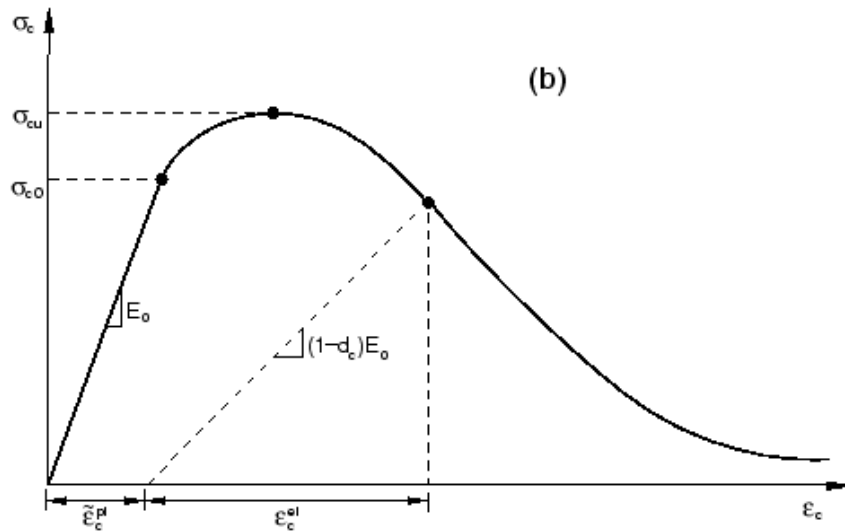

Figure 7: Response of concrete to uniaxial loading in compression (ABAQUS 2013)

Cracks tend to propagate in the direction normal to the direction of stress. Cracks normally initiate in the direction of maximum shear stress then propagate in the direction of maximum principal stress. In the following equations the E_{0ijkl} is the initial or undamaged elastic stiffness of the material. The stress-strain relationship is then defined by ABAQUS per the following equations

$$\sigma_{tij} = (1-d_t)E_{0ijkl}\left(\varepsilon_{tij} - \tilde{\varepsilon}_{tij}^{p}\right) \tag{1-9}$$

$$\sigma_{cij} = (1-d_c)E_{0ijkl}\left(\varepsilon_{cij} - \tilde{\varepsilon}_{cij}^{p}\right) \tag{1-10}$$

Then concrete nucleates a crack and the crack then propagates the load carrying capacity of the concrete is reduced due to the reduction in load carrying capacity of the area. The crack reduces the area capable of providing strength and this strength reduction needs to be accounted for in the numerical model. The modulus of elasticity of the material, which is the essence of the numerical stiffness model, is also reduced as follows

$$E_{ijkl} = (1-d)E_{0ijkl} \qquad (1\text{-}11)$$

where the undamaged or initial modulus of elasticity of the concrete is defined as E_{0ijkl}. Since concrete can have degradation at any one time due to both tension and compression the damage parameter is determine as follows

$$(1-d) = (1-s_t d_t)(1-s_c d_c) \qquad 0 \le s_t, s_c \le 1 \qquad (1\text{-}12)$$

Using this information the ABAQUS model can be created and the material properties of the constitutive components can be assembled as accurately as possible.

Several test panels were created for both testing and analysis. The two panels that will be discussed briefly here have significant importance to the overall research and development. The first panel is the solid concrete test panel and FEA model. This panel is shown in Figure 8 and has only concrete and reinforcing steel parts.
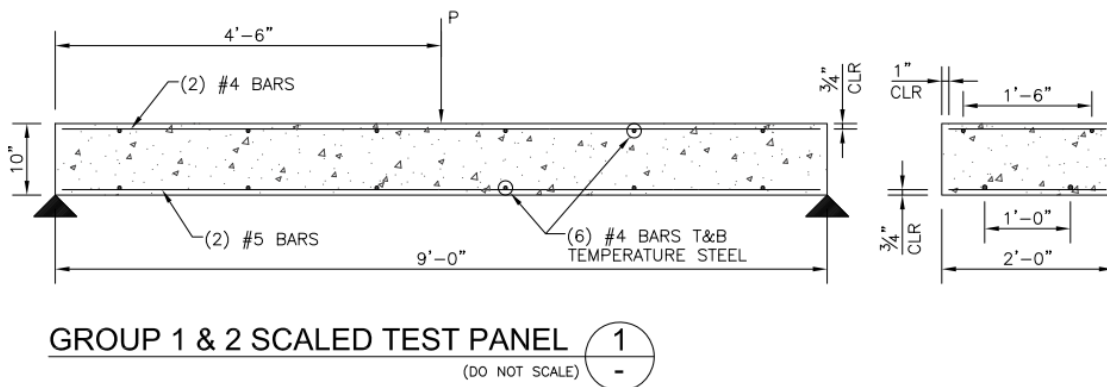

Figure 8: 10" solid concrete panel construction

By using the material properties and the damaged plasticity model in ABAQUS the FEA model and the test results matched quite well and with ease in both linear elastic and nonlinear portions of the loading curve. Figure 9 shows the comparison between the two test panels and the two FEA models. The only difference in the FEA models was the size of the element, which went from 2 inch hexahedral elements to 1 inch hexahedral elements.
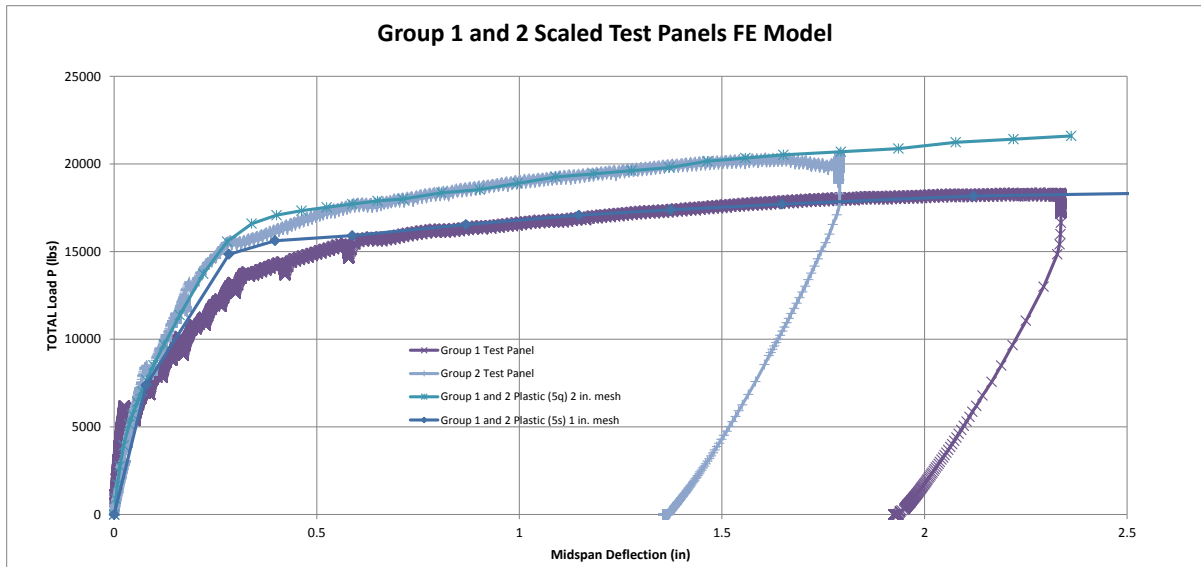
Figure 9: 10" solid concrete panel FEA vs. Test results

Once a working numerical modeling technique for the solid concrete panel had been established, the sandwich panel FEA model was then developed. Based on the construction geometry of the 10-inch panel with segmental FRP connectors as shown in Figure 10 a FEA model was then created. Once again the material properties of the constitutive materials and linear hexahedral linear elements with an element size of about 1 inch were used.
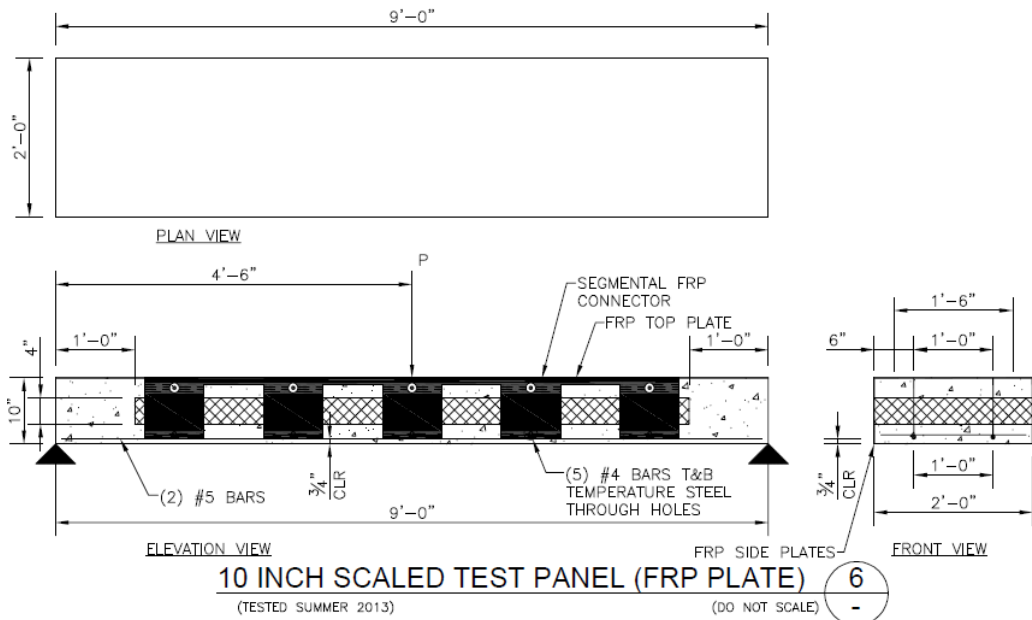

Figure 10: 10"Segmental FRP panel with top and side FRP plates

After reviewing the FEA results for the 10-inch segmental FRP panel with and without the FRP top and side plates and then comparing those results to the solid concrete panels, there are positive indications that the sandwich panel with FRP plates can provide the level of strength and serviceability desired. Figure 11 shows the test and

FEA results for the solid concrete panel, the 10-inch sandwich panel with FRP top and side plates and the 10-inch sandwich panel with no side plates. Once again the FEA and test results match well and the 10-inch sandwich panel with FFP plates can provide comparable strength to that of the solid concrete panel, while providing the insulation properties and less weight.
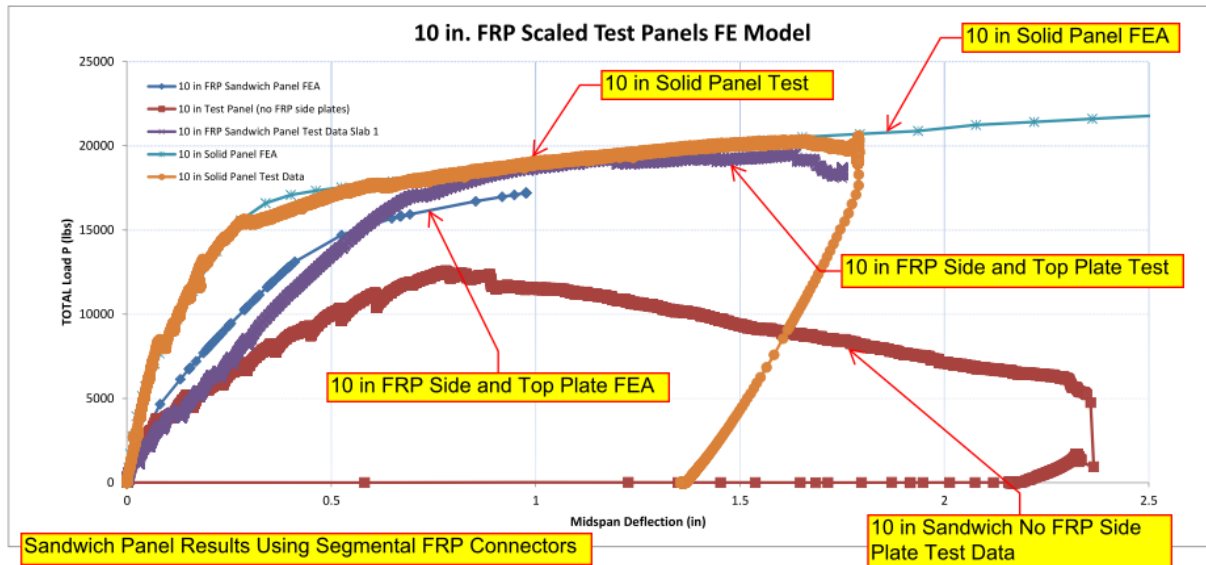

Figure 11: Overall FEA vs. Testing comparison with various panels

The FEA model can show the tension and compression damage or stiffness degradation in the panel at incremental load steps. The tension damage just prior to failure, or when the tension zone crosses into the compression zone, is shown in Figure 12. The tension damage at total failure is then shown in Figure 12, where the severe nonlinearity of the numerical model is obvious.
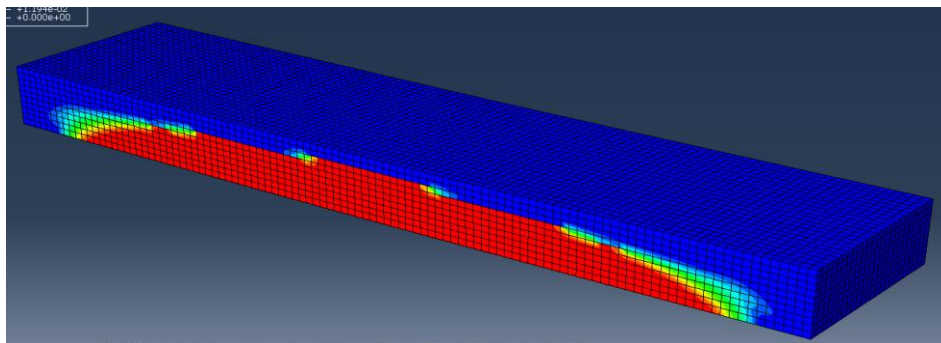

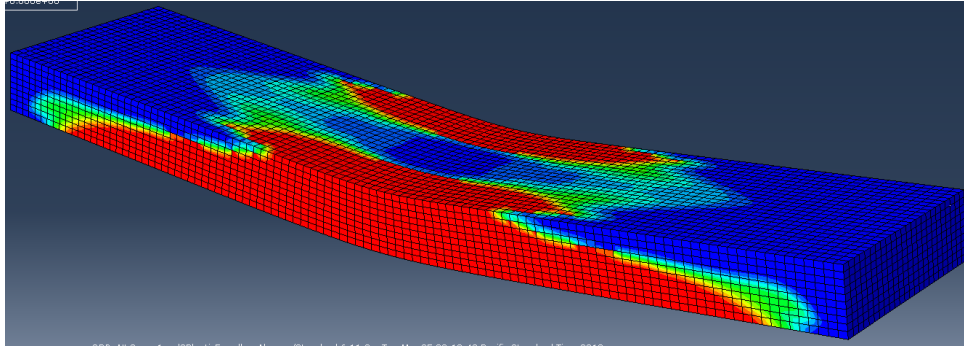**Figure 12: Tension damage in solid concrete panel at near failure**

Figure 13: Tension damage in solid concrete panel at total failure

Guided by the FE results, a comprehensive experimental investigation was carried out, including bending tests on scaled specimens with different shear connectors and with or without external FRP plates, bending tests on full-scale specimen, and creep tests on scaled specimens, as described next.

1.2.2   *Bending tests of scaled specimens:*

Bending tests on sixteen scaled specimens were conducted to determine the optimum shear connector in Phase 1 and study the effect of external FRP plates in Phase 2.

PHASE 1: Scaled Specimens with different types of shear connectors:

Eight slabs were fabricated and tested included two solid panels and six sandwich panels. The specimens were 10 inch deep, 2 ft wide, and 9 ft long. The sandwich panels consisted of three layers from top to bottom: top concrete wythe, foam core, and bottom concrete wythe, as shown in Figure 14. Three types of shear connectors were studied, including discrete shear connectors, continuous shear connectors and segmental shear connectors (see Figure 15, Figure 16, Figure 17, respectively). Table 3 lists details for each specimen.
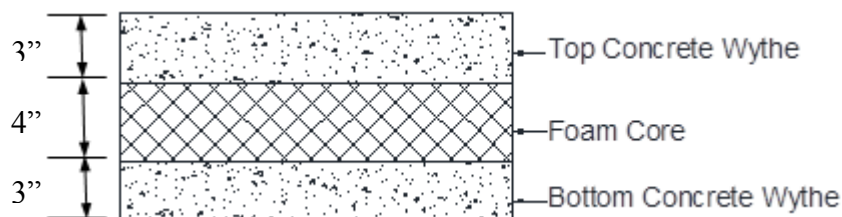

Figure 14: Sandwich Panel

Table 3: Phase 1 - Specimen Details

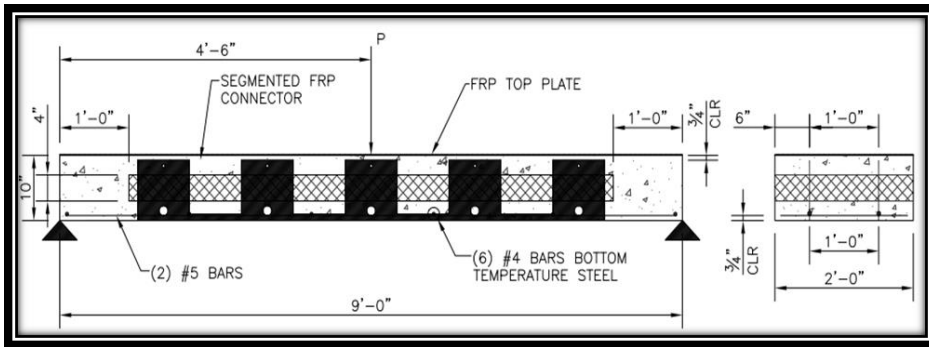| Group #	Compression Steel (#4 bars)	Tension Steel (#5 bars)	Top Temp. Steel (#4 bars)	Bottom Temp. Steel (#4 bars)	Load Condition	Shear Connectors
1	(2) @ 18" O.C.	(2) @ 12" O.C.	(6) @ 18" O.C.	(6) @ 18" O.C.	3-pt Bending	N/A
2	(2) @ 18" O.C.	(2) @ 12" O.C.	(6) @ 18" O.C.	(6) @ 18" O.C.	3-pt Bending	N/A
3	(2) @ 18" O.C.	(2) @ 12" O.C.	(6) @ 18" O.C.	(6) @ 18" O.C.	4-pt Bending	Discrete 6"
4	(2) @ 18" O.C.	(2) @ 12" O.C.	(6) @ 18" O.C.	(6) @ 18" O.C.	4-pt Bending	Discrete 6"
5	(2) @ 18" O.C.	(2) @ 12" O.C.	(6) @ 18" O.C.	(6) @ 18" O.C.	3-pt Bending	Segmental
6	(2) @ 18" O.C.	(2) @ 12" O.C.	(6) @ 18" O.C.	(6) @ 18" O.C.	3-pt Bending	Segmental
7	(2) @ 18" O.C.	(2) @ 12" O.C.	(6) @ 18" O.C.	(6) @ 18" O.C.	3-pt Bending	Continuous
8	(2) @ 18" O.C.	(2) @ 12" O.C.	(6) @ 18" O.C.	(6) @ 18" O.C.	3-pt Bending	Continuous
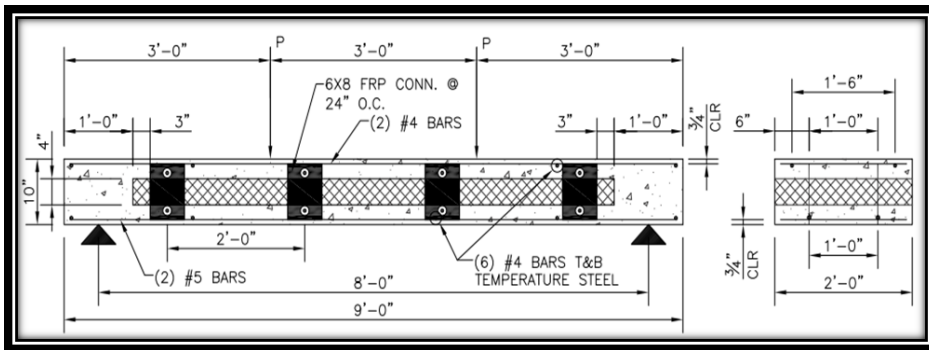
Figure 15: Discrete Shear Connector Layout

Figure 16: Segmental Shear Connector Layout

Figure 17: Continuous Shear Connector Layout

Three-point bending tests were conducted, with a schematic plan of the test setup shown in Figure 18. Strain gages were bonded along the depth of the specimen to study composite behavior. Load-displacement relation was recorded to study stiffness. All specimens were tested until failure to study strength and failure modes. The specimens either failed due to bending failure or shear failure initiated from the support, as shown in Figure 19. A comparison between shear connectors can be seen in Figure 20. Table 4 provides a summary of the ultimate loads, deflections, and moments sustained by each specimen. Table 5 highlights the level of composite action achieved by each type of shear connector.

Figure 18: Schematic Test Setup

a: Bending Failure – Concrete Crushing   b: Shear Failure – Diagonal Crack
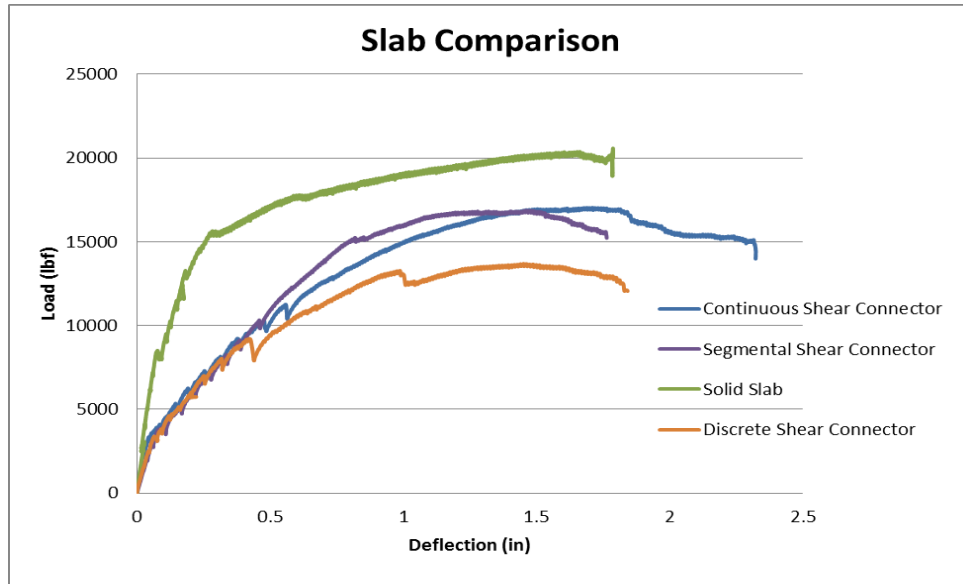
Figure 19: Failure Modes

Figure 20: Load-Displacement Comparison

Table 4: Ultimate Load Summary

Group	Cracking Load (kip)	Cracking Moment (kip*ft)	Failure Load (kip)	Failure Moment (kip*ft)	Max Load Deflection (in)
1	4	9.00	18.360	41.310	2.199
2	3	6.75	20.500	46.125	2.140
3	3	4.00	13.000	17.333	1.451
4	3	4.00	13.900	18.533	0.623
5	4	8.00	15.570	31.140	1.186
6	3	6.75	16.875	37.969	1.466
7	3	6.75	17.000	38.250	1.710
8	3	6.75	16.844	37.898	1.346

Table 5: Degree of Composite Action (DCA)

Specimen Type	Maximum Load (lbs)	Deflection (in)	DCA
Solid Slab	20600	2.14	100%
Discrete Connectors	13700	1.45	77%
Segmental Connectors	16900	1.47	93%
Continuous Connectors	17000	1.71	96%

It can be seen that the continuous shear connectors produced the highest DCA, however, the segmental shear connectors perform at a comparable level with a 26% reduction in material. Therefore, segmental shear connectors were selected for Phase 2.

PHASE 2: Bending tests of scaled specimens with external FRP plates

The next phase revolved around bending tests on eight specimens: four with top plates at 10" thick, two with top and side plates at 10" thick and two with top and side plates at 8" thick (description, sketch and photograph provided in Table 6, and Figure 21 & Figure 22, respectively). The specimens were 9 ft long and 2 ft wide, as described in Phase 1. The bottom concrete wythe was 3- inch thick. Two thicknesses of 1 inch and 3-inch were considered for top concrete wythe to be potentially used for regular roof and green roof. The two concrete wythes were separated by a 4-inch thick foam core.

Table 6: Phase 2 - Specimen Details

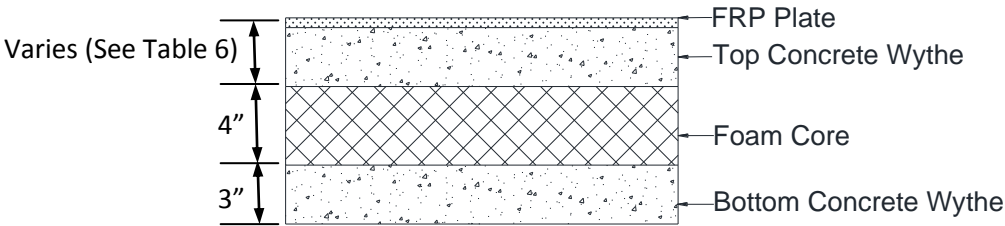| Group	Compression Steel (#4 bars)	Top Concrete Wythe	Tension Steel (#5 bars)	Top Temp. Steel (#4 bars)	Bottom Temp. Steel (#4 bars)	Top FRP Plate	Side FRP Plates
1	N/A	3"	(2) @ 12" O.C.	N/A	(6) @ 18" O.C.	Yes	No
2	N/A	3"	(2) @ 12" O.C.	N/A	(6) @ 18" O.C.	Yes	No
3	N/A	3"	(2) @ 12" O.C.	N/A	(6) @ 18" O.C.	Yes	No
4	N/A	3"	(2) @ 12" O.C.	N/A	(6) @ 18" O.C.	Yes	No
5	N/A	3"	(2) @ 12" O.C.	N/A	(6) @ 18" O.C.	Yes	Yes
6	N/A	3"	(2) @ 12" O.C.	N/A	(6) @ 18" O.C.	Yes	Yes
7	N/A	1"	(2) @ 12" O.C.	N/A	(6) @ 18" O.C.	Yes	Yes
8	N/A	1"	(2) @ 12" O.C.	N/A	(6) @ 18" O.C.	Yes	Yes

Figure 21: FPCS Panel Specimen

Figure 22: Phase 2 Testing Setup

Three-point bending tests were conducted, as described for Phase 1, with Figure 23 displaying a photo of the test in progress. Strain gages were bonded along the depth of the specimen, as well as on the shear connectors, to study composite behavior. Load-displacement relation was recorded to study stiffness. All specimens were tested until failure to study strength and failure modes. The specimens failed due to bending failure, as shown in Figure 24.

Figure 23: Test in Progress

Figure 24: Bending Failure Crack Pattern

Figure 25 provide the load-displacement curves for the Phase 2 panels. The ultimate loads and deflections of those panels can be seen in Table 7. It can be noted that the ultimate strength of 10" FPCS panel is comparable to that of the solid slab from Phase 1, yet displays a lower modulus of elasticity. Ultimately, the addition of FRP side plates resulted in an exceptional increase in strength compared to the panels with only a top FRP plate. Therefore, the addition of side FRP plates will be included in the testing of the full scale specimen.
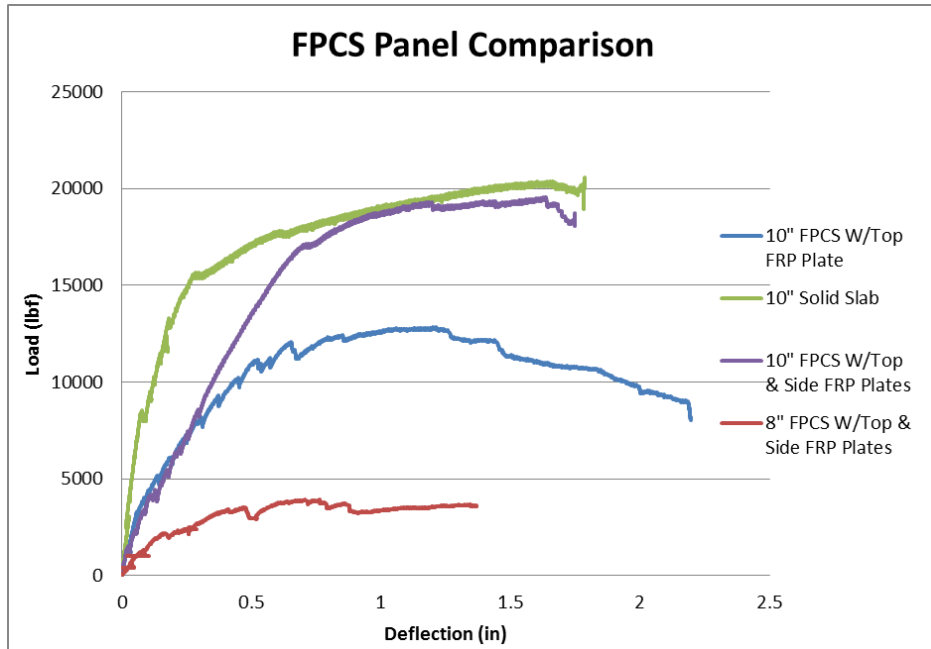

Figure 25: FPCS Panel Comparison

Group	Cracking Load (kip)	Cracking Moment (kip*ft)	Failure Load (kip)	Failure Moment (kip*ft)	Max Load Deflection (in)
1	3	6.75	12.6	28.35	0.78
2	2	4.5	12.8	28.8	1.202
3	3	6.75	15.3	34.521	1.011
4	3	6.75	16.0	36	0.779
5	2	4.5	19.6	44.1	1.636
6	3	6.75	18.8	42.3	1.088
7	3	6.75	4.5	10.125	0.361
8	3	6.75	3.9	8.775	0.705

1.2.3 Bending tests of full scale specimens w/ top & side FRP plates

Bending tests were conducted on two full scale sandwich panels with FRP plates at top and two sides. The specimens were 16 ft long and 2 ft wide. The bottom concrete wythe was 3-inch thick. Two thicknesses of 1 inch and 3 inch were considered for top concrete wythe to be potentially used for regular roof and green roof. The two concrete wythes were separated by a 4-inch thick foam core. Two specimens were tested, with one for each group.

Three-point bending tests were conducted as shown in Figure 26, with Figure 27 displaying a photo of the test in progress. Strain gages were bonded along the depth of the specimen, as well as at the shear connectors, to study composite behavior at half and quarter points. The load-displacement relation was recorded to study stiffness. All specimens were tested until failure to study strength and failure modes. The specimens failed due to bending failure, as shown in Figure 28.
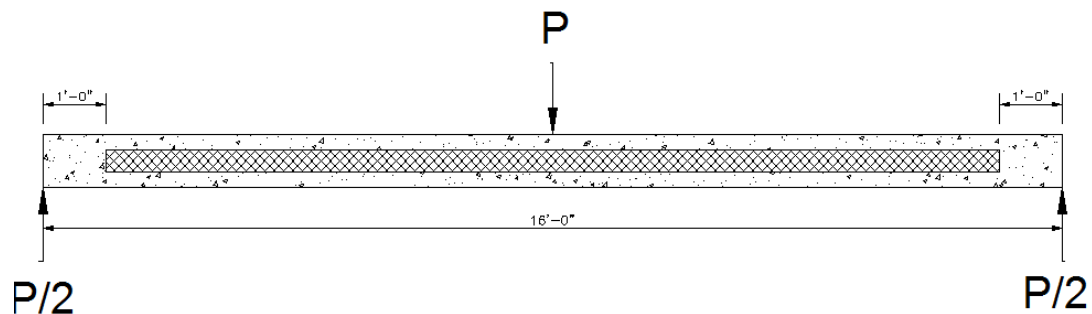

Figure 26: Full Scale Schematic Test Setup

Figure 27: Full Scale Test in Progress

Figure 28: Bending Failure

Figure 29 and Figure 30 provide load-displacement curves for the 10" and 8" slabs, respectively. The equivalent uniformly distributed load that the 10" and 8" FPCS panels could withstand were 280psf and 492psf, respectively.
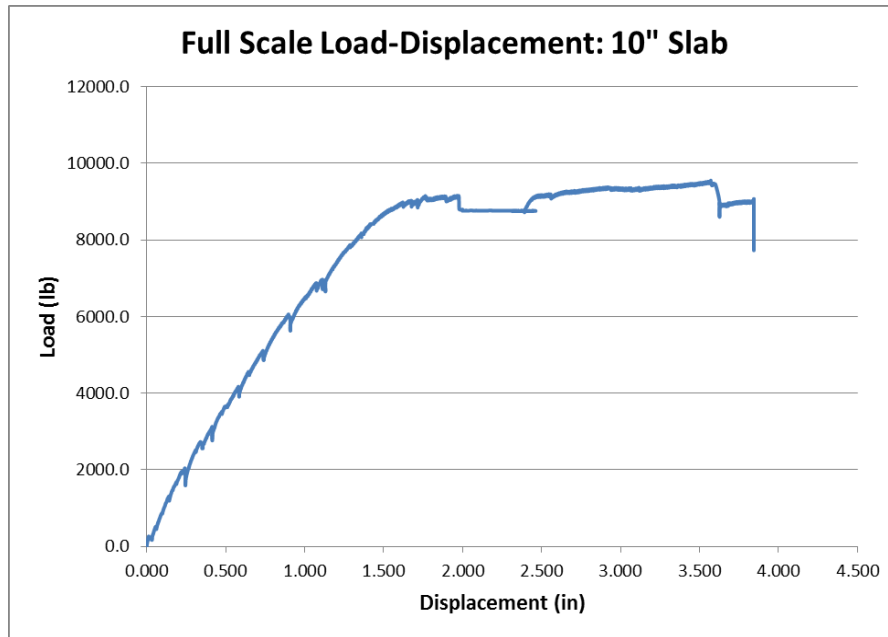
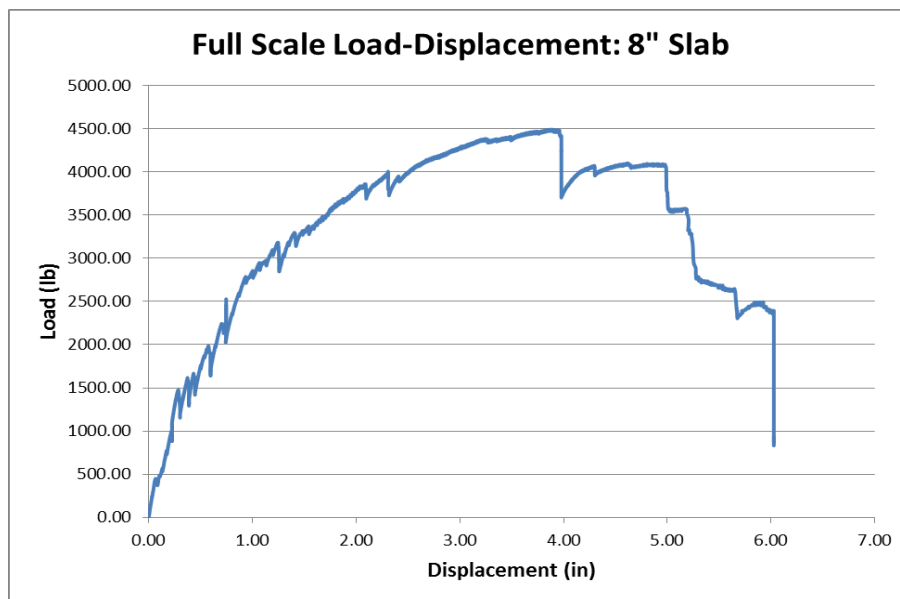**Figure 29: Full Scale Load-Displacement - 10" Slab**

Figure 30: Full Scale Load-Displacement - 8" Slab

Assuming allowable deflections of L/360 as per ACI 318-11, it was determined that the 10" FPCS panel could support service distributed floor and roof live loads of 192psf and 342psf, respectively. The 8" FPCS panels could support a service distributed floor and roof live loads of 94psf and 147psf, respectively.

1.2.4   Creep tests of scaled specimens

Creep tests are conducted to study long-term deflection of the panels under sustained loads. The same specimens as described in Phase 2 are subjected

to a four-month creep in bending at ~15% of the static capacity, as determined from the static tests. Four specimens are tested, including a solid panel, a panel without FRP plate, and two specimens as described in Phase 2 (10" and 8" slabs with top and side FRP plates).

The test is ongoing for all panels. The solid slab, sandwich panel, and 8" FPCS panel will be monitored until October 2013 (Figure 31), while the 10" FPCS panel will be monitored until the summer of 2014. All panels are monitored in strain across their depth to establish composite action. They are also monitored in deflection with gages at both quarter points and two at mid-span for each panel. The deflection curves for the solid slab, sandwich panel, 8" FPCS panel, and 10" FPCS panel can be viewed in Figures 18 – 21, respectively.
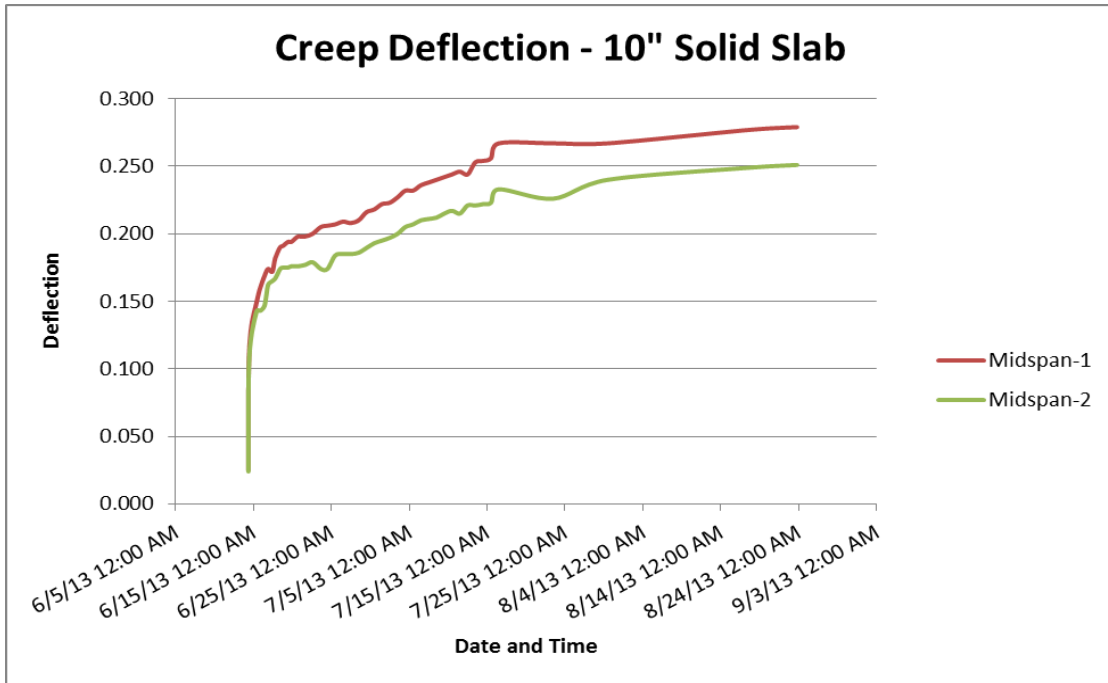

Figure 31: Creep Test Set-up

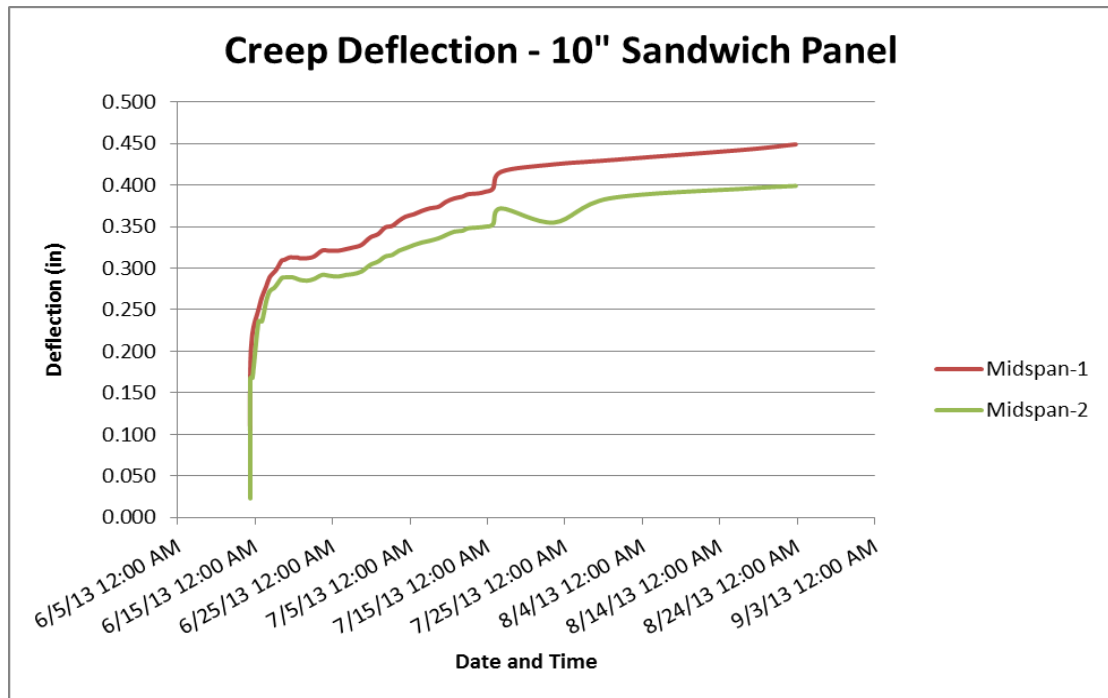**Figure 32: Mid-span Creep Deflection of Solid Slab**

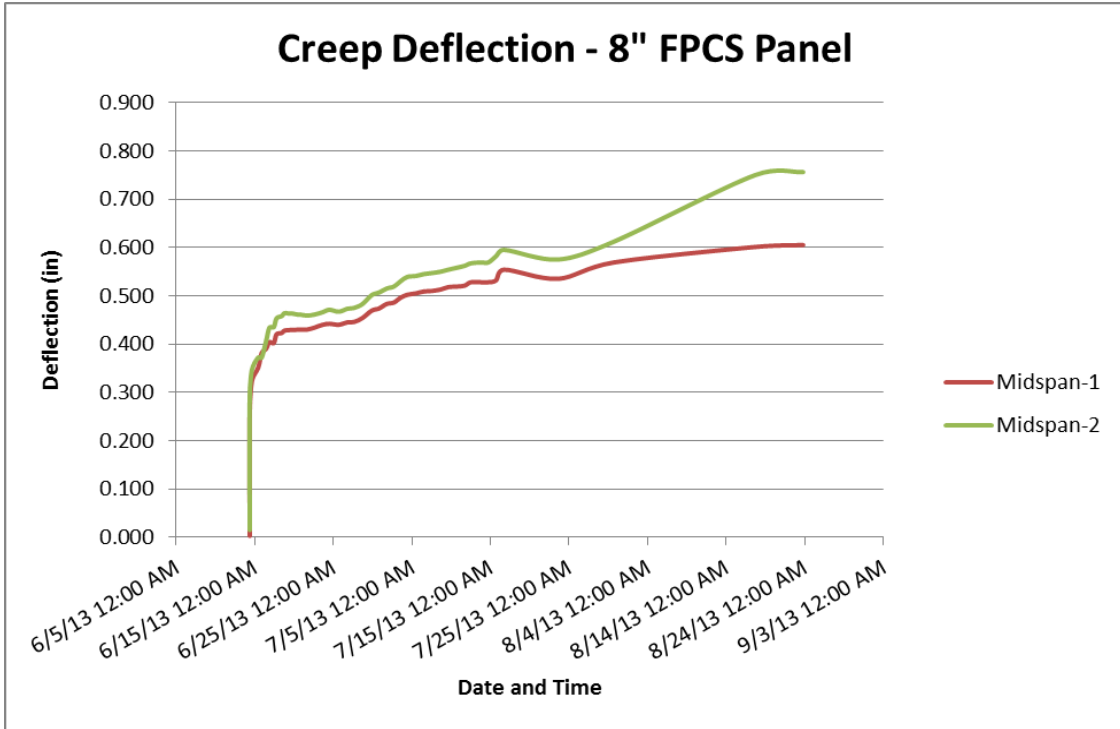**Figure 33: Mid-span Creep Deflection of Sandwich Panel**

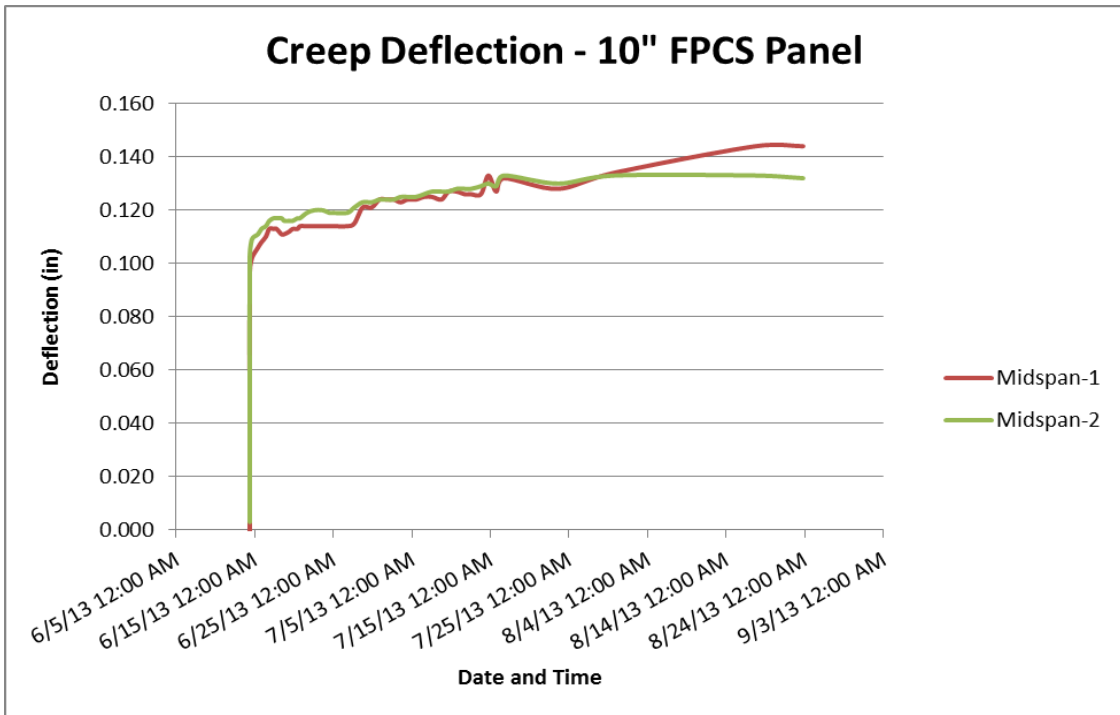**Figure 34: Mid-span Creep Deflection of 8" FPCS Panel**

Figure 35: Mid-span Creep Deflection of 10" FPCS Panel

Using this data, comparisons could be made to the full scale slabs in order to determine their sustainable loads with respect to long term deflection (see Table 8).

Table 8: Full Scale - Long-term Sustainable Loads

Specimen	Load (lbf)	Equivalent Distributed Load (psf)	Avg. Creep Deflection (in)	Equivalent Creep Deflection - Full Scale (in)	Allowable Deflection: L/480 (in)	Full Scale Sustainable Load (psf)
Solid Slab	3056	153	0.1125	0.63	0.4	97
Sandwich Panel	3082	154	0.25	1.40	0.4	44
10" FPCS	3174	159	0.138	0.78	0.4	82
8" FPCS	3137	157	0.375	2.11	0.4	30

By not exceeding these sustainable loads, these slabs would perform in accordance with ACI 318-11. Therefore, a prototype FPCS panel has been developed based on the FE and experimental investigation, which indicates it can be used for roof/floor applications.

1.2.5   Business Development Plan

The concept of FPCS panels has been proved from this research. There are some interests and inquiries from the industry, including Missouri Structural Composites, LLC and Titan Brick, Inc. However, some other requirements from International Building Code have to be met before FPCS panels can be used in roof/floor constructions. These requirements include fire, water, smoke-toxicity, etc. For example, different buildings have different fire requirements for roof panels, varying from 0 to 1-1/2 hours. These issues cannot be addressed in this research because of limited time and funding.

Currently the PI is developing a cast-in-place FRP-Confined Sandwich Roof (FCSR). This project will address the issues as described above for FPCS by developing an FRP system with improved fire, smoke-toxicity, water leakage and UV resistances. Therefore, the business plan of this research is to tie the commercialization plan of FPCS to the on-going project. Once the above issues have been resolved, the advantages of the panels are expected to attract investment. By that time, a family of products can be commercialized, including the FPCS panels (precast) from this research and FCSR (cast-in-place) from the ongoing project.

2. Describe the current state of the technology and related product/service:

Based on the comprehensive study from Section 1, a prototype FPCS roof/floor system, as shown in Figure 27, has been developed. It has been shown that composite action can be achieved based on correlations between the testing and FE results. The FPCS panels can sustain the loads from floors, standard and green roofs.

3. List the number of faculty and student participants as a result of funding:

Two faculty members, Drs. An Chen and Richard Nielsen, and three students, Paul Hopkins, Tom Norris, and Nicolas Pena participated in this project. A master's thesis, which is fully supported by this research, and a PhD dissertation, which is partly supported by this research, will be generated from this project.

4. What are the potential economic benefits:

Traditional roof systems treat roofing, insulation, and supporting structure separately. The developed technology addresses this limitation and provides an energy efficient, cost-effective, and durable structure with ease of construction. During fabrication, no concrete stripping is required, and the construction speed can be increased. During roof installation, the FPCS panel can be installed in one-step and no additional insulation layer and roofing materials are required, which can significantly reduce the construction time and cost, in particular labor cost. For conventional asphalt roofing, labor represents approximately 75% of the total cost and materials are only 25%. The insulation layer in the FPCS panel can not only significantly increase the structure's strength but also remarkably improve thermal resistance of the panel for greater thermal comfort and less energy waste. The R-value of a 10" thick FPCS panel with a 6" insulation layer is approximately 30 times greater than the value of a concrete panel with the same thickness and the same strength. Additionally, the non-steel reinforced top concrete wythe not only eliminates the potential corrosion problem associated with the steel rebars, but also provides a shield for the concrete inside the shell, expecting to significantly increase the service life of the structure. The FPCS panel is particularly suitable for green roofs, since green roofs usually have more stringent requirements for strength and water resistance.

5. Description future plans for project continuation or expansion:

Although the application of FPCS panels as roof/floor constructions has been proved from this study, multiple issues, such as fire and other requirements from the International Building Codes need to be met in order for the FPCS roof/floor system to enter building market. As a continuation and expansion of the project, the PI is currently conducting a study on a cast-in-place roof system, FCSR, to address those issues. Once completed, a family of products, FPCS (precast) and FCSR (cast-in-place) will be commercialized.

6. Please provide a final expenditure report (attached) and include any comments here:

See attached expenditure report.

7. List invention disclosures, patent, copyright and PVP applications filed, technology licenses/options signed, start-up businesses created, and industry involvement:

An international application for filing in the US receiving office has been filed on December 13, 2012, with an application number of PCT/US12/69291 and a title of *Concrete Building Panel*. There is some interest from the industry on this technology. Crane Composites, Inc. donated the FRP plates. Missouri Structural Composites, LLC provided technical support.

8. Any other pertinent information:

The research has been used as a course project to enhance the curriculum of the PI's course of CE441-Reinforced Concrete Design in Fall 2012 and create an interactive environment for students to explore concepts of reinforced concrete design through design, manufacturing, and physical experiments of the panels. 43 students from the class actively participated in the research. They were divided into 11 groups, with each group responsible for constructing and testing one panel, including rebar cutting, rebar assembling, formwork construction, concrete pouring, concrete vibrating, panel construction, form stripping, test setup, and panel testing (Figure 7). The students were able to create their own knowledge (constructivism) by an inductive experiential active learning approach, from concrete experience of experimental study (grasping experience) to abstract conceptualization of new and key theoretical aspects of reinforced concrete design (transforming experience), developing innovative and critical thinking and research ability and acquiring life-long learning qualities. The students welcomed this innovation and showed great enthusiasm in participating in this research. Responses from the students are listed below:

"After constructing a reinforced concrete slab and testing it, it gave a better understanding of the designing of reinforced concrete. It was a good opportunity to see how the reinforcements within the concrete affect the strength and durability of a slab or beam when concrete and steel are combined."

"Being able to physically see the behavior of the beam failure helped everyone in the group to better grasp the concepts covered by Dr. Chen in his class. "

"The testing of the specimen was a great way to tie in the concepts lectured throughout the course. It provided a great hands-on opportunity to apply and test our knowledge of reinforced concrete design."

"This project really helped to understand a large number of the concepts covered in CE 441 this semester. It was very interesting to see a real world application and actually get to observe the steel and concrete reach maximum stress and strain before going into failure. It is also very important to understand how certain research and testing with real world applications is completed. This project definitely gives us an advantage when entering the industry."

"The project was useful in showing us with hands-on experience how a concrete beam reacts to an increasing load, and ultimately fails. The experience of recognizing cracks forming and the significance of where and when they occur can only be helpful in the future. It was also interesting to observe the tension and compression reinforcement as it reached its yield strain. Testing of the reinforced concrete beam was helpful in creating a better understanding of reinforced concrete design."

"The experiments performed in the lab allowed hands on learning approach. This is helpful for students with different learning styles and allows for experimental results, not only showing the expected deflection and nominal moment capacity but through a linear observation of the failure mode. The inclusion of structural experiments in a structures design class can greatly enhance a student's retention."

a: Rebar Cutting   **b: Rebar Assembling**   **c: Formwork Construction**

d: Concrete Pouring   **e: Concrete Vibrating**

f: Surface Smoothing **g: Constructed Panels** **h: De-molded Panels**

i: Test Setup **j: Panel Testing**

k: Panel Failure **l: Failure Mode**

Figure 36: Students' Participation

One abstract was published by ASCE Engineering Mechanics Institute Conference (EMI2013), which was held in August 2013 in Chicago. As a training process, two students attended the conferences and presented the abstract. Some journal papers are in preparation and expected to be submitted soon.

Acknowledgements

A. FACULTY AND STAFF		
Name/Title	$ Amount Requested	Actual $ Spent
An Chen	9,000	8,208

B. VISITING PROFESSORS		
Name/Title	$ Amount Requested	Actual $ Spent

C. POST DOCTORAL ASSOCIATES/OTHER PROFESSIONALS		
Name/Title	$ Amount Requested	Actual $ Spent

D. GRADUATE/UNDERGRADUATE STUDENTS		
Name/Title	$ Amount Requested	Actual $ Spent
Thomas Norris/MS student	20,800	20,252 (Salary: 13440; Tuition: 6812)
Nicolas Pena/undergraduate research assistant, Christopher Davidson/student helper, Nick Kuish/student helper, Michaela Peterson/student helper, Gregory Reince/student helper	7,300	7,951

E. FRINGE BENEFITS		
Rate of Fringe (%)	$ Amount Requested	Actual $ Spent
Project director/ Graduate/Undergraduate Research Assistants	3,000	2,850
PERSONNEL SUBTOTAL:	**40,100**	39,261

F. EQUIPMENT: (List each item with a cost in excess of $1000)		
Item/Description	$ Amount Requested	Actual $ Spent
1		
2.		
3.		
4.		
EQUIPMENT SUBTOTAL:		

G. TRAVEL		
Description	$ Amount Requested	Actual $ Spent
1. Travel – Thomas Norris	2,800	100
2.		
3		
TRAVEL SUBTOTAL:	2,800	100

H. PARTICIPANT SUPPORT COSTS:		
Description	$ Amount Requested	Actual $ Spent
1.		
2.		
3		
PARTICIPANT SUPPORT COSTS SUBTOTAL:		

I. OTHER DIRECT COSTS:			
Description		$ Amount Requested	Actual $ Spent
1.Materials and supplies		5,600	8,839
2.Computer software license		1,500	1,800
3.			
OTHER DIRECT COSTS SUBTOTAL:		7,100	10,639
TOTAL COSTS (Add Subtotals):		50,000	50,000
TOTAL AMOUNT REQUESTED:			50,000
TOTAL AMOUNT SPENT:			50,000